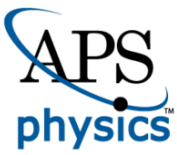

Topological ferroelectric phases by mode-selective phonon excitation

Huaxiang Fu

Phys. Rev. B **98**, 134111 — Published 23 October 2018

DOI: 10.1103/PhysRevB.98.134111

Topological ferroelectric phases by mode-selective phonon excitation

Huaxiang Fu
Department of Physics, University of Arkansas, Fayetteville, Arkansas 72701, USA
(Dated: October 8, 2018)

Topological structural phases (TSP) of nontrivial winding number are of long-standing fundamental relevance in the theory of phase transition. However, for decades, no TSP have been discovered in technological ferroelectric bulk solids. Here we formulate a generally-applicable scheme to create TSP in ferroelectrics. The approach consists in selectively exciting phonon modes to produce the targeted TSP, and can be employed to generate novel TSP that do not naturally exist in bulk materials. We further demonstrate the effectiveness of this approach by creating in bulk $SrTiO_3$ three TSP structures, namely the flower, tetragonal-like vortex, and orthorhombic-like vortex phases. These topological phases lead to the discovery of interesting properties, which include (i) a marked difference in the excitation stiffness of different topological phases, and (ii) the existence of symmetry breaking between vortex phases.

Topological structural phases (TSP) have widespread importance, ranging from Quantum Hall state[1, 2], spin-lattice skyrmion[3], to two-dimensional gravity[4]. Hence generating unusual TSP has been a topic of profound interest for decades.[5] Among them, TSP—that can be generated when solids are under external excitation and yet do not exist under ambient condition—are of particular relevance both fundamentally and technologically. Fundamentally, these TSP do not naturally exist in ambient solids, and therefore can vastly expand (and deepen) the existing knowledge of unknown structural phases. Furthermore, controlled by external excitations, these TSP may thus be turned on and off, which allows the occurrence of unconventional phase transitions and drastic tuning of properties. Moreover, the interatomic interaction in TSP could be profoundly different from that in bulk solids, providing microscopic insights to study structure formation and structure transformation. Technologically, solids in TSP often display superior properties which are absent in normal solids, and hence offer promise for new applications. For examples, under X-ray illumination, $Pr_{0.7}Ca_{0.3}MnO_3$ was discovered to undergo pronounced phase transition from insulator to metallic ferromagnetic state, displaying colossal magnetoresistence.[6, 7] Similarly, an enhanced superconductivity was reported in $YBa_2Cu_3O_{6.5}$ when the solid is under terahertz optical pulse.[8]

According to the theory of topology, topological structural phases are characterized by the topological winding number, defined as the number of 2π by which a vector-field order parameter rotates after having travelled a loop of closed path.[5, 9] When the winding number is nonzero, a topologically nontrivial structural phase exists, which is distinct from, and cannot be continuously deformed into, a topologically trivial phase.[5, 9]

Ferroelectrics (FE) are an important class of solids with spontaneous polarization[10], caused by the delicate balance between long-range Coulomb and short-range covalent interactions[11]. The large dielectric response[12], ultrahigh electromechanical coefficients[13, 14], existence of unusual morphotropic phase boundary[15–18], strong polarization proximity effect[19], and large coupling between rotation and polarization[20–23] make them unique for various applications.

In ferroelectrics, different phases are often obtained by varying temperature. Structural phases such as cubic, monoclinic, tetragonal, orthorhombic, and rhombohedral phases may be achieved by change of temperature.[10] However, the winding numbers of these phases are all zero,[5] and are hence topologically trivial. Another route of obtaining different structural phases in ferroelectrics is to utilize the depolarization field in the low-dimensional structures [24–29]; this approach is to be named the "depolarization-field approach" (DFA). Obviously these low-dimensional phases in FE nanostructures depend critically on the existence of depolarization field. DFA nevertheless has two limitations: (i) The depolarization field is hard to control precisely; (ii) In bulk solids where depolarization fields vanish, this approach does not apply.

Here we propose and implement a different approach to create topologically nontrivial structure phases in ferroelectrics, which can vastly increase the number of previously unknown structural phases. Unlike previous approach of DFA [24–27], the current approach does *not* require the existence of depolarization field, and is generally applicable for any ferroelectrics even when there is completely no depolarization field. The present method is rigorous and consists in generating the desired TSP by excitation of selective phonon modes. To demonstrate the validity of our method, we go one step further and successfully apply the approach to *bulk* $SrTiO_3$ (STO) in which no depolarization field occurs, producing novel structural phases that do not exist in bulk STO, such as the flower state (which, to our knowledge, has not yet been experimentally realized in ferroelectric bulks and/or nanostructures.)

Furthermore, as one marked feature of importance, the current approach allows to control the displacements of individual atoms. We find in this study that excitation of a combination of X_5 mode at 129.3 cm^{-1} and X_1 mode at 284.5 cm^{-1} in $SrTiO_3$ generates a FE vortex (of winding number 1) in which Ti atoms move along the *tetragonal* direction, and in contrast, excitation of X_5 mode at

129.3 cm^{-1} alone nevertheless gives rise to a remarkably-different FE vortex in which Ti atoms move along the *orthorhombic* direction. Moreover, our study reveals intriguing physics about ferroelectric TSP: (i) There is a possibility that phase transformation may exist between different ferroelectric states of curled polarization; (ii) Two similar TSP states could have surprisingly different energetics. Combinations of these results demonstrate that there is interesting and rich physics to be learnt about TSP in ferroelectrics.

Let us first describe the topological ferroelectric phases that we intend to generate; none of these phases exist in bulk $SrTiO_3$. We begin with $SrTiO_3$ at room temperature (which is cubic), and intend to create topologically nontrivial structures within $2 \times 2 \times 1$ supercell. Furthermore, we require that the displacements of Ti atoms in TSP form unusual patterns as displayed in Fig.1(a)-(c). The reason we choose to work with $SrTiO_3$ at room temperature is that the costly cooling process becomes unnecessary for creating TSP. The TSP in Fig.1(a)-(c) exhibit the following features: (i) The Ti atoms in Fig.1(a) move collectively toward the center of the supercell, forming a flower state. This state is to be abbreviated as the "F" state. (ii) The Ti atoms in Fig.1(b) are simultaneously displaced along the $\langle 100 \rangle$-equivalent directions in the respective bulk cell of each Ti atom, forming a polarization vortex phase. In this phase, since each Ti atom moves toward the "tetragonal" direction, this vortex state will be named as the tetragonal-like vortex state, to be denoted as "T_V state". (iii) The Ti atoms in Fig.1(c) form another vortex-like state; unlike the vortex state in Fig.1(b), the Ti atoms in Fig.1(c) move along the $\langle 110 \rangle$-equivalent directions (which is to be named as an orthorhombic-like vortex state, abbreviated as "O_V state").

Here it worths pointing out that at this moment we only know the displacements of Ti atoms, and the positions where Sr and O atoms will be located are not yet known. The displacements of those atoms other than Ti must be determined by the principle of constrained energy minimization. Furthermore, we would like to emphasize that, unlike in FE nanostructures or at FE interfaces[28, 29], there is no depolarization field in FE bulks, and therefore, generating topological FE phases or vortex-like FE ordering with nonzero topological winding number in *bulk* (such as the T_V and O_V phases in Fig.1) is highly nontrivial. Although interesting electric skyrmions and other topological phases were recently proposed in multi-domain solids[30], very few topological ferroelectric phases have been discovered so far in single-domain bulks where depolarization field vanishes.

Our approach consists of three steps. The validity of these steps is confirmed by many TSP we have generated, in addition to those in Fig.1. First, we determine where other atoms should be located in response to the designated topological pattern of Ti displacements, by performing a constrained first-principles total-energy optimization in which the positions of Ti atoms are constrained. This is done by the density functional theory[31] (DFT). It leads to the optimized positions of other atoms within the constrained subspace, which should lower the excitation energy for the targeted TSP. Denote the atomic positions after optimization as $r'_{\rm opt}(l'\zeta'\alpha)$, where l' is cell index, ζ' is atom index within a cell, α is the direction index of cartesian coordinate. Since TSP is often a super-structure with different lattice periodicity than the bulk solid [e.g., as in Fig.1(a)-(c)], we denote the periodic lattice of the TSP *super-structure* as $\vec{R}'_{l'} = l'_1\vec{a}'_1 + l'_2\vec{a}'_2 + l'_3\vec{a}'_3$, where l'_i are integers, and $\vec{a}'_1 = 2a_0\vec{i}$, $\vec{a}'_2 = 2a_0\vec{j}$, and $\vec{a}'_3 = a_0\vec{k}$ are lattice vectors of TSP (with a_0 being the lattice constant of cubic $SrTiO_3$, and $\vec{i}$, $\vec{j}$, $\vec{k}$ being unit vectors along the cubic [100], [010], [001] directions). Meanwhile, denote the periodic lattice of *bulk* as $\vec{R}_l = l_1\vec{a}_1 + l_2\vec{a}_2 + l_3\vec{a}_3$ (where $\vec{a}_1 = a_0\vec{i}$, $\vec{a}_2 = a_0\vec{j}$, and $\vec{a}_3 = a_0\vec{k}$ are the lattice vectors of bulk). Symbols with prime describe quantities belonging to the TSP super-structure, and symbols without prime describe quantities belonging to bulk.[32]

From the optimized atomic positions $r'_{\rm opt}(l'\zeta'\alpha)$ obtained in constrained minimization, we determine the atomic displacements of the TSP super-structure with respect to the centrosymmetric configuration of zero polarization as $d'(l'\zeta'\alpha) = r'_{\rm opt}(l'\zeta'\alpha) - r'_{\rm c}(l'\zeta'\alpha)$, where $r'_{\rm c}(l'\zeta'\alpha)$ is the atomic position of centrosymmetric configuration. We further construct a normalized vector as $e'(l'\zeta'\alpha) = \frac{1}{A}\sqrt{\frac{M_{\zeta'}}{N'}}d'(l'\zeta'\alpha)$, in which $|A|^2 = \frac{1}{N'}\sum_{l'\zeta'\alpha} M_{\zeta'}\,|d'(l'\zeta'\alpha)|^2$ is the normalization factor, $M_{\zeta'}$ is atomic mass, and N' is the number of TSP supercells in the solid.

Second, we use linear response perturbation theory[34–36] to determine for bulk solids the phonon eigenmodes $e_{n\vec{k}}(l\zeta\alpha)$ and phonon displacements $[u_{n\vec{k}}(l\zeta\alpha) = \frac{1}{\sqrt{M_\zeta}}e_{n\vec{k}}(\zeta\alpha)e^{i\vec{k}\cdot\vec{R}_l}]$ at branch n and wave vector $\vec{k}$. We then project the vector $e'(l'\zeta'\alpha)$ of the super-structure of TSP using the phonon displacements $u_{n\vec{k}}(l\zeta\alpha)$ of bulk as

$$e'(l'\zeta'\alpha) = \sum_{n\vec{k}} C_{n\vec{k}} \left\{ \sqrt{\frac{M_\zeta}{N}} u_{n\vec{k}}(l\zeta\alpha) \right\} \quad , \qquad (1)$$

in which $l'\zeta'\alpha$ and $l\zeta\alpha$ correspond to the same displacement direction of the same atom. N is the number of bulk cells in the solid. Eq.(1) is possible since displacements $u_{n\vec{k}}(l\zeta\alpha)$ of bulk phonons at different $n\vec{k}$ form a complete basis. Using the orthonormal properties $\frac{1}{N}\sum_{l\zeta\alpha} M_\zeta\, u^*_{n_1\vec{k}_1}(l\zeta\alpha)\, u_{n\vec{k}}(l\zeta\alpha) = \delta_{n_1 n}\delta_{\vec{k}_1\vec{k}}$, one can determine $C_{n\vec{k}}$ as

$$C_{n\vec{k}} = \sum_{l\zeta\alpha} \sqrt{\frac{M_\zeta}{N}} u^*_{n\vec{k}}(l\zeta\alpha) e'(l'\zeta'\alpha) \quad . \qquad (2)$$

$C_{n\vec{k}}$ reveals which phonon modes need be excited in order to form the desired TSP. It is straightforward to prove that $C_{n\vec{k}}$ satisfy the identity equation $\sum_{n\vec{k}} |C_{n\vec{k}}|^2 = 1$, which is also confirmed in our numerical calculations.

As a third step, we reconstruct new TSP with atomic displacements $\tilde{d}'(l'\zeta'\alpha)$ by selectively exciting a subset of nonzero-$C_{n\vec{k}}$ bulk phonons according to

$$\sqrt{\frac{M_{\zeta'}}{N'}}\tilde{d}'(l'\zeta'\alpha) = \sum_{n\vec{k}} Q_{n\vec{k}} C_{n\vec{k}} \left\{ \sqrt{\frac{M_\zeta}{N}} u_{n\vec{k}}(l\zeta\alpha) \right\} \quad , \quad (3)$$

where excitation weight $Q_{n\vec{k}}$ can be chosen by adjustment of the excitation intensity at different $n\vec{k}$. If $Q_{n\vec{k}}$ is chosen to be uniform (i.e., $Q_{n\vec{k}} = Q$), the desired TSP is obtained. If $Q_{n\vec{k}}$ is chosen to be inhomogeneous (i.e., $Q_{n\vec{k}}$ depends on $n\vec{k}$), other TSP structures of sub-group symmetry will be obtained.

Technically we perform the constrained structural optimization using first-principles density functional theory within the local density approximation (LDA) via QUANTUM ESPRESSO.[37, 38] Norm-conserving pseudopotentials of Troullier-Martins type[39] are used to account for the effects of core electrons. Semi-core states of Ti $3s$ and $3p$ are treated as valence states to ensure better accuracy.[40] The cut-off energy for wave function expansion is 100Ry, which was found sufficient in calculations of various properties such as lattice vibration under finite electric fields[41], effects of vacancies[42], and rigorous computing of LO/TO splitting[43]. To determine phonon frequencies and eigenmodes, we use density functional perturbation theory[34, 35] (DFPT) and linear response calculations, in which the perturbation-induced changes in wavefuntions are obtained by solving the Sternheimer equation $(H_{scf}-\varepsilon_n)|\Delta\psi_n\rangle = -(\Delta V_{scf} - \Delta\varepsilon_n)|\psi_n\rangle$, where H_{scf} is the Kohn-Sham Hamiltonian of unperturbed system, ε_n is single-particle eigenvalue of H_{scf}, and $\Delta V_{scf}(\mathbf{r}) = \Delta V(\mathbf{r}) + e\int \frac{\Delta n(\mathbf{r}')}{|\mathbf{r}-\mathbf{r}'|}\,\mathrm{d}\mathbf{r}' + \left.\frac{dv_{xc}(n)}{dn}\right|_{n=n(\mathbf{r})} \Delta n(\mathbf{r})$ is the self-consistent perturbation potential. With atomic displacements of a topological structure phase (obtained from constrained structural optimization) and bulk-phonon eigenmodes (obtained from linear response calculations), two in-house computation codes are written to perform phonon projection and to reconstruct new topological structures generated by selective excitation of phonon modes.

The atomic displacements, obtained from constrained DFT structural optimization, are shown in Fig.1(a)-(c) for the F, T_V, and O_V phases, respectively. During the structural optimization only the displacements of Ti atoms are constrained, while other atoms are allowed to relax. For all three considered TSP in Fig.1, we find that the displacements of Sr atoms are rather small and are thus not shown.

Fig.1(a)-(c) reveals two interesting observations: (i) In the F phase (Fig.1a) and T_V phase (Fig.1b), despite the fact that the Ti displacements are drastically different (namely they are centripetal in the F phase, but are circularly rotating in the T_V phase), the displacement patterns of O1-O4 atoms are nevertheless remarkably similar, and in particular, all of them move toward the center of the $2\times2\times1$ supercell, showing that different patterns of Ti displacements may lead to surprisingly similar patterns in O displacements. This plays an important role in determining the energetics of topological ferroelectric phases (see below). (ii) On the other hand, although the Ti displacements in T_V and O_V phases (Fig.1b and Fig.1c) are similar—and in both phases are circularly rotating, the displacements of O atoms are, however, notably unlike. Interestingly, while the displacements of O1-O4 atoms in Fig.1c form a vortex, the displacements of O1-O4 in Fig.1b do not. The fact that the O1-O4 atoms do not form a vortex in Fig.1b also demonstrates that the local off-center displacements of atoms may considerably differ from the global topology of TSP. It is thus unjustified to assume that the displacements of each atomic species are conformed with the global topology.

As described above, topological structural phases can be characterized by the topological winding number. Examining the displacement vectors of Ti on a circle connecting the four Ti atoms in Fig.1(a)-(c), it is straightforward that the winding numbers of all three structural phases are +1.[5, 9] Therefore, the F, T_V, and O_V phases are topologically nontrivial structures, which are stable as long as excitation remains.

We have also determined the topological winding numbers of the considered TSP, by computing the local polarization of each 5-atom bulk cell, defined as $\vec{P}_{\rm loc}(c) = \frac{1}{\Omega}\sum_{i\epsilon c} Z_i^* \Delta\vec{r}_i$, where c is the index for 5-atom bulk cells, i is the atom index, Ω is the volume of a bulk cell, Z_i^* is the Born effective charge tensor, and $\Delta\vec{r}_i$ is the displacement of atom i. Since the three topological phases all have a four-fold C_4 rotation symmetry, the local $\vec{P}_{\rm loc}(c)$ polarizations of the four bulk cells in Fig.1(a)-(c) are symmetry related. We will thus present $\vec{P}_{\rm loc}(c)$ in the bulk cell at the bottom left of the supercell in Fig.1(a)-(c), and this bulk cell is to be called bulk cell I.

We find that, for the O_V phase in Fig.1(c), when the magnitude of Ti displacement is 0.1 Å, the local polarization in bulk cell I is $\vec{P}_{\rm loc} = (0.118, -0.118, 0)$ C/m^2, where the Cartesian x, y, z directions are along the cubic [100], [010], [001] axes, respectively. This tells that (i) $\vec{P}_{\rm loc}$ is nonzero, and each bulk cell is thus ferroelectric; (ii) $\vec{P}_{\rm loc}$ points at the direction of Ti displacement in the cell; (iii) After using the C_4 symmetry, we find that the topological winding number for the O_V phase, obtained from the $\vec{P}_{\rm loc}$ polarizations, is +1 in Fig.1(c) (which is the same as that obtained from the Ti-displacement vectors), showing that the phase is indeed topologically nontrivial. Similar conclusions are also valid for the F and T_V phases, where the local polarization in bulk cell I is $\vec{P}_{\rm loc} = (0.083, 0.083, 0)$ C/m^2 for the F phase and $\vec{P}_{\rm loc} = (0.157, -0.039, 0)$ C/m^2 for the T_V phase, when the magnitude of Ti displacement is 0.1 Å.

It is worthy of noticing that the vortex size of Ti displacements in Fig.1(b) and (c) is markedly small—only four bulk cells with a length of merely 0.77nm, which is smallest ferroelectric vortex that has been discovered so

far (to the best of our knowledge). The tiny FE vortices found in Fig.1 promise to produce an ultrahigh density of ferroelectric memories on the order of 10^3 Terabits/inch^2, which is approaching the ultimate limit of FRAM.[44]

The vortices obtained in Fig.1 for *bulk* solids differ profoundly from the FE vortices previously reported in FE *nanodots*[28], in two important aspects: (1) The FE vortex in nanodots was determined using effective Hamiltonian which involves only soft mode. Since a soft mode consists of a frozen amount of contribution from each individual atom in bulk cell[45], the displacements of each species of atoms (such as O) therefore also form a vortex. In contrast, the FE vortex, obtained from *ab initio* calculations, reveals that the displacements of individual species do *not* necessarily form a vortex as demonstrated by the O atoms in Fig.1(b), which will significantly alter both lattice and electronic properties. (2) Our results show that FE vortex does not even need to originate from soft modes. For instance, in T_V phase (Fig.1b), the peculiar displacements of the Ti and O1 atoms in the top-left cell are not related to the soft mode at Γ or the rotational-instability mode at M.

We next turn attention to determining what phonon modes and at which specific $\vec{k}$ points in bulk $SrTiO_3$ need be excited in order to generate the topological phases in Fig.1(a)-(c). By using the group theory of translational symmetry,[46] we find that only the lattice-vibration modes at two phonon wave vectors in bulk $SrTiO_3$, namely $\vec{k}_1 = \frac{2\pi}{a}(0, \frac{1}{2}, 0)$ and $\vec{k}_2 = \frac{2\pi}{a}(\frac{1}{2}, 0, 0)$, contribute to forming the topological F, T_V and O_V phases, which is consistent with the fact that the supercells of these phases have a lattice periodicity of $2 \times 2 \times 1$. Since $\vec{k}_1$ and $\vec{k}_2$ are symmetry equivalent, we will mainly focus our discussion on $\vec{k}_1$.

The bulk phonon modes at $\vec{k}_1$ are $2X_{5'} \oplus 3X_5 \oplus 2X_{4'} \oplus X_2 \oplus 2X_1$, according to the irreducible representation of group theory. The $X_{5'}$ and X_5 are doubly degenerate, and other modes are singly degenerate. The frequencies of bulk phonons at $\vec{k}_1$, obtained from our linear response calculations, are 108.4 and 318.5 for two $X_{5'}$ modes, 129.3, 174.4, and 527.4 for three X_5 modes, 170.4 and 776.1 for two $X_{4'}$ modes, 281.1 for X_2, 284.5 and 542.5 for two X_1 modes (all frequencies are in units of cm^{-1}). These mode frequencies are plotted in Fig.2(a).

The modes—that need be excited at $\vec{k}_1$ in order to generate each considered TSP—and their quantitative $|C_{n\vec{k}}|^2$ contributions are shown in Fig.2(b)-(d). For the sake of visualization, the $|C_{n\vec{k}}|^2$ contributions in Fig.2(b)-(d) are Gaussian broadened, with a broadening width of 5.25 cm^{-1}. After excitation, it is numerically confirmed by Eq.(3) that the computed atomic displacements exactly match those TSP in Fig.1(a)-(c).

Rather remarkably we find that, to generate the unusual TSP, no complicated phonon excitations are needed. Instead, a *few* modes are sufficient to meet the goal. According to our calculations, to create the flower (F) state, only a predominating X_1 mode at frequency ω=284.5 cm^{-1}, with a minor contribution from another X_1 mode at ω=542.5 cm^{-1}, is needed (see Fig.2b). Even the complex T_V phase and the O_V phase with peculiar atomic-displacement patterns also require only a few modes: two predominating modes (X_5 at 129.3 cm^{-1} and X_1 at 284.5 cm^{-1}) need be excited in order to generate the T_V phase (Fig.2c),[47] and to produce the O_V phase, one predominating mode (X_5 at 129.3 cm^{-1}) is sufficient (Fig.2d).

Selective excitation of phonon modes cannot be achieved by temperature, since thermal excitation is random, and will affect all phonons at every wave vector. The random excitation is cancelled and will not cause TSP. To generate TSP, one possible approach is to use neutrons of definite energy and momentum. By momentum and energy conservations, one can excite specific vibration modes at specific phonon wave vectors.

It is interesting that the F phase is formed by exciting the *singly* degenerated X_1 modes (Fig.2b). But the O_V phase must be created by exciting the *doubly* degenerated X_5 modes (Fig.2d). Furthermore, since both T_V and O_V phases are vortex-like structures and have similar Ti-displacement patterns (Fig.1), intuition tells us that their phonon modes of excitation should be similar. However, Fig.2c and Fig.2d reveal that the excitations to generate the T_V and O_V phases are notably different. Unlike the O_V phase that requires only doubly-degenerate X_5 excitation (Fig.2d), the T_V phase is formed by mixing the doublet X_5 and singlet X_1 modes (and both components are significant in Fig.2c).

The difference in the mode excitations of three topological phases originates from the fundamental difference in crystallographical symmetry. By examining the space group of atomic positions,[48] we have identified the crystal symmetry of each TSP. We find that the F phase has a symmorphic crystal symmetry of P4/mmm (space group 123); the T_V phase has a symmorphic crystal symmetry of P4/m (space group 83); the O_V phase has a non-symmorphic crystal symmetry of P4/mbm (space group 127). The two circularly-polarized phases (T_V and O_V) are thus found to have different crystal symmetries. This finding is of important implication for the following reason. It is known that one key criterion of judging whether or not a phase transition exists is by the breaking of symmetry.[49] Since the T_V and O_V phases have different symmetries, the transformation between these vortices is thus a phase transition.

Two possible approaches may realize the transition from the O_V to T_V phases: (i) One approach is by rotating the Ti displacements from the orthorhombic direction to the tetragonal direction. This can be achieved by excitation of additional phonons (which rotate the Ti displacements) or by external electric fields. (ii) Another approach is to utilize the intermediate cubic phase, by first turning off the phonon excitation of the O_V phase so that the structure returns to the cubic phase, and then turning on the phonon excitation of the T_V phase which will make the structure transform from the cubic phase

to the T_V phase.

Switching of a topological vortex state is also possible. Consider a FE vortex state with toroid moment $+\vec{G}$. Its degenerate state is a vortex with an opposite toroid moment -$\vec{G}$. Switching can be realized by turning off the phonon excitation of $+\vec{G}$ (so that the system is transformed to the cubic phase) and then turning on the phonon excitation of -$\vec{G}$ (so that the toroid moment is switched).

We now investigate the energetics of different topological phases. Here we are interested in the uniform excitation, namely the circumstance that $Q_{n\vec{k}}$ in Eq.(3) is a constant ($Q_{n\vec{k}} = Q$) independent of $n\vec{k}$, which perhaps is the most important scenario that can be implemented in experiments by uniformly adjusting the excitation intensity. Obviously the energy to excite a TSP depends on the amplitude Q, for Q describes how far the TSP deviates from the unexcited structure. Fig.1(d) depicts the excitation energies as a function of Q for three considered TSP, obtained from DFT total-energy calculations on the TSP reconstructed using Eq.(3).

We numerically find that the excitation energy can be well described analytically by formula $\Delta E = a_2Q^2 + a_4Q^4 + a_6Q^6$, which is witnessed by the fitting curves in Fig.1(d). Another merit of this analytical expression is that it yields quantitatively the stiffness of topological excitation, characterized by the a_2 coefficient. The obtained a_2, a_4 and a_6 coefficients are respectively 2.8209, 0.1987, 0.0067 eV for the F phase; 1.8282, 0.4187, -0.0157 eV for the T_V phase; and 0.4748, 0.4857, -0.0949 eV for the O_V phase. These coefficients reveal that the stiffness of the F phase is the highest among the three phases, with its a_2 value to be nearly 600% times that of the O_V phase. In contrast, the O_V phase is soft, requiring the least excitation energy. Furthermore, our first-principles results predict that, for the O_V phase, the higher-order a_4 coefficient is significant (and in fact, is comparable with a_2), showing that the anharmonic effect is particularly important for this phase.

Without excitation of phonons, the ground state of $SrTiO_3$ at room temperature is cubic (the energy of which is denoted as E_0), and the TSP are not the lowest energy state and will have a finite lifetime before relaxing to the ground state. However, with the excitation of phonons, the energy E_{ext} of external excitation (i.e., the sum of the energies of all phonons excited) is absorbed by $SrTiO_3$. After absorption, the total energy of $SrTiO_3$ is $E_0 + E_{ext}$. With respect to $E_0 + E_{ext}$, the TSP have a lower energy, and are stable as long as the excitation remains.

It is straightforward that the F phase in Fig.1(d) should have a high excitation energy since, by moving concentrically toward the center of supercell, Ti ions which are positively charged will trigger strong Coulomb repulsion and thus increase the energy.

However, it is rather surprising that the energy of the T_V phase in Fig.1(d) is markedly higher, by over 100%, than that of the O_V phase for a given Q. Both being circularly-polarized and possessing similar Ti-displacement patterns (Fig.1b and c), the T_V and O_V phases are anticipated to exhibit similar excitation energetics. But our *ab initio* results show otherwise, which is interesting and meanwhile puzzling.

We now provide microscopic insight to explain the considerable difference in energy between the T_V and O_V phases. The difference can be understood by the subtlety in local environment and local depolarization field. Note that the O displacements form a vortex-like structure in the O_V phase (Fig.1c), but not in the T_V phase (Fig.1b). In T_V phase (Fig.1b), although Ti displacements are vortex-like, the O displacements display instead an unusual head-to-head pattern. This head-to-head O pattern gives rise to strong local depolarization field and increases the energy, which explains why the T_V phase has significantly higher energy than the O_V phase.

The relative energetics of three TSP in Fig.1(d) are consistent with the outcome of phonon excitations. As revealed in Fig.2(b)-(d), the (high-energy) F phase mainly consists of the excitation of X_1 mode at a *high* frequency of 284.5 cm^{-1}—and in contrast, the (low-energy) O_V phase consists of predominantly the excitation of the X_5 mode at a *lower* frequency (129.3 cm^{-1}). It signals a correlation between the energy of TSP and the frequencies of phonon modes that need be excited, as it should.

The current approach of generating TSP offers considerable advantages. (a) In *bulk* FEs, structure phases are often obtained by varying temperatures.[10] However, the number of structural phases that can be obtained by temperature is rather limited. Only a handful of structural phases such as cubic, tetragonal, monclinic, orthorhombic, and rhombohedral phases have been achieved. In contrast, the method implemented in this study can generate many novel structure phases that do not exist in bulks. (b) The current method of generating TSP is superior than the previous DFA approach of utilizing depolarization, for depolarization fields are difficult to control. Furthermore, since the current approach of phonon excitation applies to any bulk FEs, it can thus vastly expand the range of materials that host topological ferroelectric phases. DFA does not work for bulk. (c) Although phase transformations between two structures of different polarizations (e.g., between rhombohedral and tetragonal phases via polarization rotation[13, 14]) have been amply studied, transitions between two topological FE phases with nonzero winding numbers are far less explored. This may open a new field to study phase transformations, which should broaden our knowledge on the fundamental theory of phase transition.

In summary we have formulated a scheme to generate technologically-important and topologically-nontrivial structure phases in ferroelectrics by selective excitation of phonon modes. The approach (i) can be applied to any ferroelectrics and is thus general; (ii) is able to create novel and previously unknown structure phases that

do not naturally exist in bulk FEs, which allows fundamental knowledge to be gained on atomic interactions in new phases; (iii) is rigorous since bulk phonon modes are complete in forming any topological structures.

By taking a step further and implementing the method on $SrTiO_3$, we discovered that only a very few modes are needed in order to generate the F, T_V, and O_V phases, which are topological phases with winding number of 1. Among them, the F phase has not yet been experimentally realized in either bulk FEs or nanostructured FEs, and meanwhile, the T_V and O_V phases are smallest ferroelectric vortices found thus far, promising for ultrahigh density of ferroelectric memories. Our results show that (1) FE vortex phases need not result from soft modes, and (2) individual species of atoms (e.g. O atoms) may defy conventional wisdom by not possessing vortex-like displacements in vortex phase.

We further demonstrated a marked difference in the excitation stiffness between the T_V and O_V phases. The difference can be microscopically attributed to local depolarization field caused by the head-to-head oxygen displacements in the T_V phase, revealing the critical importance of local structure. Moreover, the T_V and O_V phases are found having distinct symmetry, signaling that transformation between different topological phases is thus a new type of phase transitions. Based on the fact that topologically nontrivial structure phases in ferroelectrics are fundamentally interesting and poorly understood, we hope that the current study will stimulate more theoretical and experimental interest in this exciting field.

This work was supported by the Office of Naval Research. The computing facility was provided by the High-Performance Computing Center at the University of Arkansas.

[1] D.J. Thouless, M. Kohmoto, M.P. Nightingale, and M. den Nijs, Phys. Rev. Lett. **49**, 405 (1982).

[2] F.D.M. Haldane, Phys. Rev. Lett. **61**, 2015 (1988).

[3] S. Muhlbauer, B. Binz, F. Jonietz, C. Pfleiderer, A. Rosch, A. Neubauer, R. Georgii, and P. Boni, Science **323**, 915 (2009).

[4] E. Witten, Nuclear Phys. B **340**, 281 (1990).

[5] N.D. Mermin, Rev. Mod. Phys. **51**, 591 (1979).

[6] V. Kiryukhin, D. Casa, J.P. Hill, B. Keimer, A. Vigliante, Y. Tomioka, and Y. Tokura, Nature **386**, 813 (1997).

[7] M. Fiebig, K. Miyano, Y. Tomioka, and Y. Tokura, Science **280**, 1925 (1998).

[8] R. Mankowsky, A. Subedi, M. Forst, S.O. Mariager, M. Chollet, H.T. Lemke, J.S. Robinson, J.M. Glownia, M.P. Minitti, A. Frano, M. Fechner, N.A. Spaldin, T. Loew, B. Keimer, A. Georges, and A. Cavalleri, Nature **516**, 71 (2014).

[9] M. Nakahara, *Geometry, topology and physics* (Tylor & Francis, New York, 2003).

[10] M.E. Lines and A.M. Glass, *Principles and Applications of Ferroelectrics and Related Materials* (Clarendon, Oxford, 1979).

[11] R. E. Cohen, Nature (London) **358**, 136 (1992); R. E. Cohen and H. Krakauer, Phys. Rev. B **42**, 6416 (1990).

[12] A.M. George, J. Iniguez, and L. Bellaiche, Nature (London) **413**, 54 (2001).

[13] S.-E. Park and T.R. Shrout, J. Appl. Phys. **82**, 1804 (1997).

[14] H. Fu and R.E. Cohen, Nature (London) **403**, 281 (2000).

[15] B. Noheda, D.E. Cox, G. Shirane, J.A. Gonzalo, L.E. Cross, and S.-E. Park, Appl. Phys. Lett. **74**, 2059 (1999).

[16] B. Noheda, D.E. Cox, G. Shirane, S.-E. Park, L.E. Cross, and Z. Zhong, Phys. Rev. Lett. **86**, 3891 (2001).

[17] X. Fu, I.I. Naumov, and H. Fu, Nano. Lett. **13**, 491 (2012).

[18] I. Naumov and H. Fu, Phys. Rev. Lett. **98**, 077603 (2007); Phys. Rev. Lett. **101**, 197601 (2008).

[19] J.B. Neaton and K.M. Rabe, Appl. Phys. Lett. **82**, 1586 (2003).

[20] C.J. Fennie and K.M. Rabe, Phys. Rev. B **72**, 100103(R) (2005).

[21] E. Bousquet, M. Dawber, N. Stucki, C. Lichtensteiger, P. Hermet, S. Gariglio, J.-M. Triscone, and P. Ghosez, Nature (London) **452**, 732 (2008).

[22] N.A. Benedek and C.J. Fennie, Phys. Rev. Lett. **106**, 107204 (2011).

[23] J.M. Rondinelli and C.J. Fennie, Adv. Mater. **24**, 1961 (2012).

[24] M. Dawber, K.M. Rabe, and J.F. Scott, Rev. Mod. Phys. **77**, 1083 (2005).

[25] S.K. Streiffer, J.A. Eastman, D.D. Fong, C. Thompson, A. Munkholm, M.V. Ramana Murty, O. Auciello, G.R. Bai, and G.B. Stephenson, Phys. Rev. Lett. **89**, 067601 (2002).

[26] D.D. Fong, G.B. Stephenson, S.K. Streiffer, J.A. Eastman, O. Auciello, P.H. Fuoss, and C. Thompson, Science **304**, 1650 (2004).

[27] I.I. Naumov, L. Bellaiche, and H. Fu, Nature **432**, 737 (2004).

[28] H. Fu, *Unusual properties of nanoscale ferroelectrics*, in "The Oxford Handbook of Nanoscience and Technoloy", Volume II (edited by A.V. Narikar), Page 688 (Oxford University Press, 2010).

[29] A.K. Yadav, C.T. Nelson, S.L. Hsu, Z. Hong, J.D. Clarkson, C.M. Schleptz, A.R. Damodaran, P. Shafer, E. Arenholz, L.R. Dedon, D. Chen, A. Vishwanath, A.M. Minor, L.Q. Chen, J.F. Scott, L.W. Martin, and R. Ramesh, Nature **530**, 198 (2016).

[30] M.A.P. Goncalves, C. Escorihuela-Sayalero, P. Garcia-Fernandez, J. Junquera, and J. Iniguez, arxiv1806.01617.

[31] P. Hohenberg and W. Kohn, Phys. Rev. **136**, B864 (1964); W. Kohn and L.J. Sham, Phys. Rev. **140**, A1133 (1965).

[32] In the theory of lattice dynamics (Ref.33), atomic positions are often described in terms of real-space lattice vectors, i.e., $\vec{r}_i = \vec{R}_l + \vec{t}_i$. In this study, we need atomic locations both in TSP and in bulk, where two crystal structures have different lattice vectors. Therefore, for a given atom, there are two ways to describe its position: (i) Using the lattice vectors $\vec{a}'_1$, $\vec{a}'_2$, and $\vec{a}'_3$ of the

TSP supercell, which is the primed coordinate. (ii) Using the lattice vectors $\vec{a}_1$, $\vec{a}_2$, and $\vec{a}_3$ of bulk, which is the unprimed coordinate. Take the undisplaced O1 atom in Fig.1a as an example. Set the origins of both primed and unprimed coodinates to be at the Sr atom at the center of the supercell in Fig.1a. Then, in the primed coordinates, the atomic position of O1 is $\vec{r}_i\,' = \vec{R}'_{l'} + \vec{t}_i\,'$, with $\vec{R}'_{l'} = 0\vec{a}'_1 + 0\vec{a}'_2 + 0\vec{a}'_3$ and $\vec{t}_i\,' = -0.25\vec{a}'_1 + 0\vec{a}'_2 + 0.5\vec{a}'_3$. In the unprimed coordinates, the atomic position of O1 is $\vec{r}_i = \vec{R}_l + \vec{t}_i$, with $\vec{R}_l = -\vec{a}_1 + 0\vec{a}_2 + 0\vec{a}_3$ and $\vec{t}_i = 0.5\vec{a}_1 + 0\vec{a}_2 + 0.5\vec{a}_3$.

[33] M. Born and K. Huang, *Dynamical theory of crystal lattices*, (Oxford University Press, Oxford, 1988).

[34] S. Baroni, S. de Gironcoli, A. Dal Corso, and P. Giannozzi, Rev. Mod. Phys. **73**, 515 (2001).

[35] S. Baroni, P. Giannozzi, and A. Testa, Phys. Rev. Lett. **58**, 1861 (1987).

[36] X. Gonze, Phys. Rev. A **52**, 1096 (1995).

[37] P. Giannozzi, S. Baroni, N. Bonini, M. Calandra, R. Car, C. Cavazzoni, D. Ceresoli, G.L. Chiarotti, M. Cococcioni, I. Dabo, A.D. Corso, S.d. Gironcoli, S. Fabris, G. Fratesi, R. Gebauer, U. Gerstmann, C. Gougoussis, A. Kokalj, M. Lazzeri, L. Martin-Samos, N. Marzari, F. Mauri, R. Mazzarello, S. Paolini, A. Pasquarello, L. Paulatto, C. Sbraccia, S. Scandolo, G. Sclauzero, A.P. Seitsonen, A. Smogunov, P. Umari, and R.M. Wentzcovitch, J. Phys. C **21**, 395502 (2009).

[38] http://www.quantum-espresso.org.

[39] N. Troullier and J. L. Martins, Phys. Rev. B **43**, 1993 (1991).

[40] H. Fu and O. Gulseren, Phys. Rev. B **66**, 214114 (2002).

[41] I.I. Naumov and H. Fu, Phys. Rev. B **72**, 012304 (2005).

[42] A. Raeliarijaona and H. Fu, Sci. Rep. **7**, 41301 (2017).

[43] A. Raeliarijaona and H. Fu, Phys. Rev. B **92**, 094303 (2015).

[44] J.F. Scott, *Ferroelectric memories* (Springer, Berlin, 2000).

[45] W. Zhong, D. Vanderbilt, and K.M. Rabe, Phys. Rev. Lett. **73**, 1861 (1994); R.D. King-Smith and D. Vanderbilt, Phys. Rev. B **49**, 5828 (1994).

[46] M.S. Dresselhaus, G. Dresselhaus, and A. Jorio, *Group Theory* (Springer-Verlag, Berlin, 2010).

[47] The mode displacements of doublet X_5 phonons at frequency 129.3cm^{-1} are $(0, -0.996, 0, -0.021, 0.082)$ along the x- and z-directions respectively for (Sr,Ti,O1,O2,O3) at $\vec{k}_1$. The mode displacements of the singlet X_1 phonon at frequency 284.5cm^{-1} are $(0, 0.422, 0, 0.641, 0.641)$ along the y-direction respectively for (Sr,Ti,O1,O2,O3). O3 is the apical oxygen in an oxygen octahedron.

[48] The ISOTROPY software suite (http://stokes.byu.edu/iso/isotropy.php).

[49] L.D. Landau and E.M. Lifshitz, *Statistical Physics* (Pergamon, NY, 1980), Part 1.

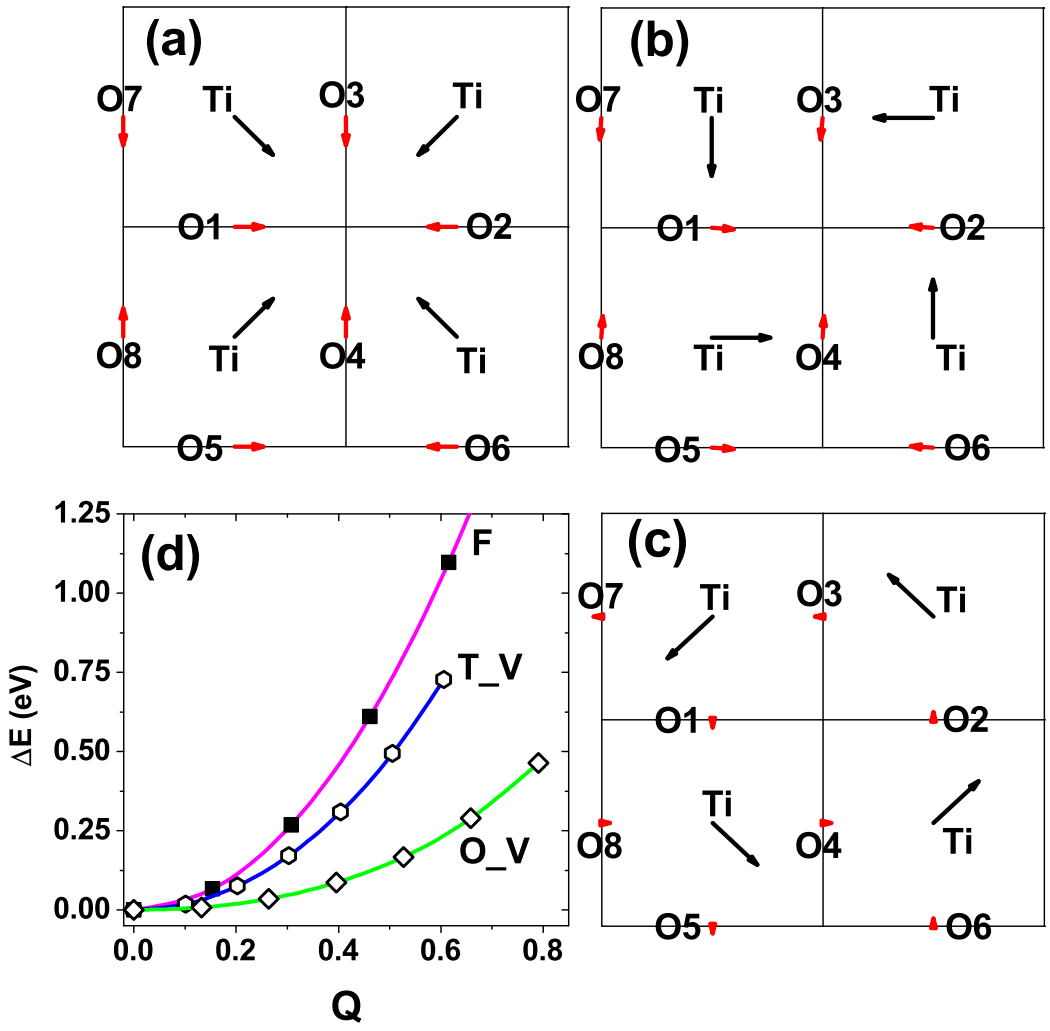

FIG. 1: Top view (along the crystallographic $[00\bar{1}]$ direction of perovskites) of the atomic displacements on the TiO_2 plane, for the following topological structure phases: (a) the F phase, (b) the T_V phase, and (c) the O_V phase. The locations of O atoms in (a)-(c) are labelled for the sake of discussion. The total energy as a function of excitation amplitude Q is shown in (d). In (d), symbols are results obtained from direct DFT calculations using the atomic positions reconstructed from Eq.(3), and curves are obtained from analytical fitting.

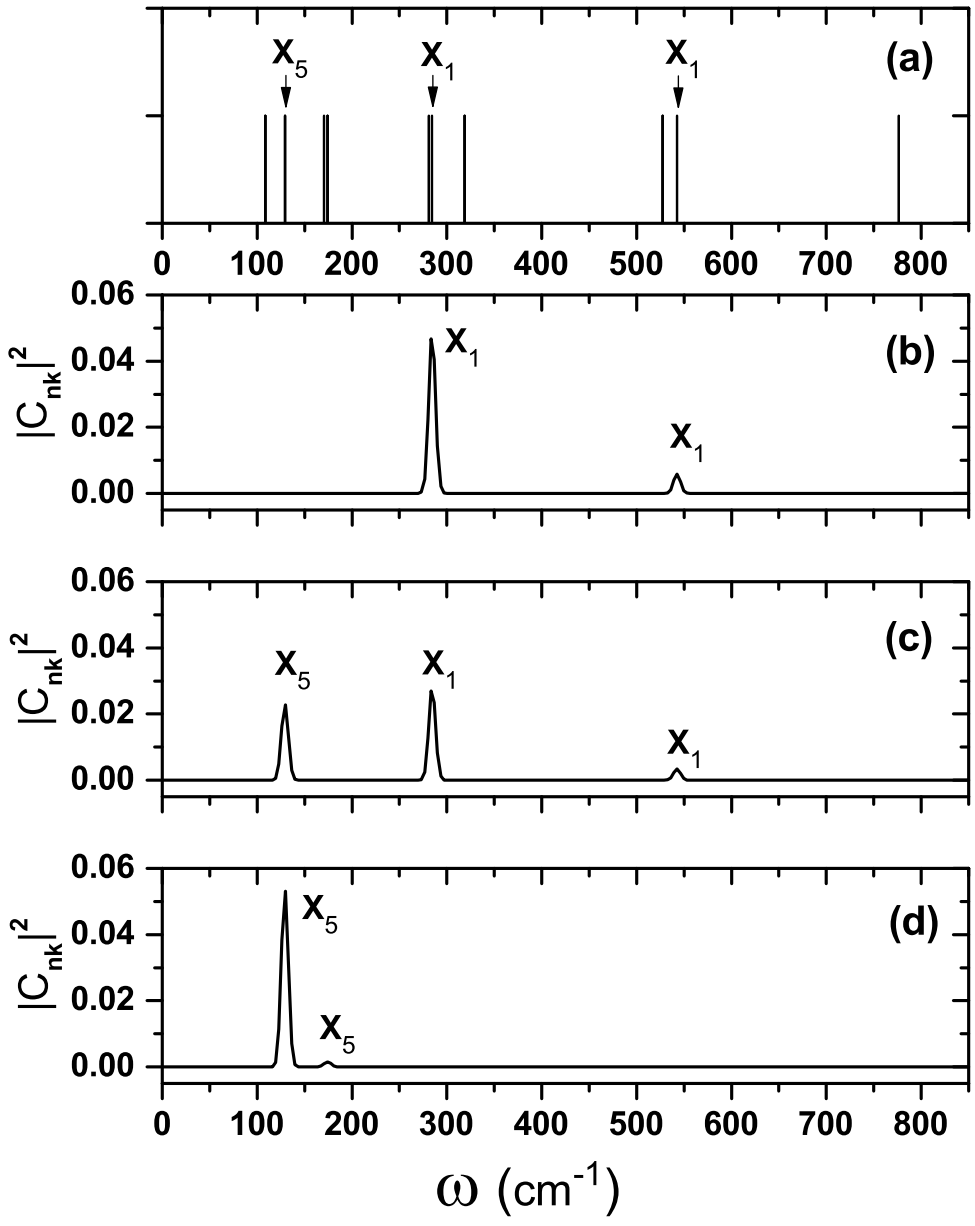

FIG. 2: (a) The ω frequencies (in cm^{-1}) of phonon modes at $\vec{k}_1$ in bulk $SrTiO_3$, as indicated by the positions of vertical lines. (b)-(d) The $|C_{n\vec{k}}|^2$ contributions of individual phonon modes at $\vec{k}_1$ to the formation of the following topological structure phases: (b) the F phase, (c) the T_V phase, and (d) the O_V phase.